

Computation of Finite Time Lyapunov Exponents using the Perron-Frobenius operator

P. Tallapragada

Abstract

The problem of phase space transport which is of interest both theoretically and from the point of view of applications has been investigated extensively using geometric and probabilistic methods. Two of the important tools for this that emerged in the last decade are the Finite time Lyapunov exponents (FTLE) and the Perron-Frobenius operator. The relationship between these approaches has not been clearly understood so far. In this paper a methodology is presented to compute the FTLE from the Perron-Frobenius operator, thus providing a step towards combining both the methods into a common framework.

1 Introduction

The problem of phase space transport has important applications such as in mixing and separation problems in fluid flows that vary in scale from the micro to the geophysical, interplanetary transport and instability of mechanical systems, to name a few. A variety of dynamical systems methods have been studied over the past three decades to explain transport mechanisms, to detect barriers to transport, and to quantify transport rates, see eg [1], [2], [3], [4], [5], [6], [7], [8], [9], [10], [11]. These methods fall into two main categories, the geometric and the probabilistic. Under the umbrella of geometric methods are the techniques of invariant manifolds (of fixed points), lobe dynamics and Finite time Lyapunov exponents (FTLE) and Lagrangian coherent structures (LCS). The method of FTLE and LCS has proven to be particularly useful in studying transport in time dependent systems and has found a variety of applications, for e.g., [12], [13], [14], [15], [16] and [17]. The probabilistic approach studies the transport of densities and the so called almost invariant sets and coherent sets. These methods too have been successfully applied in the study of various geophysical flow problems, [10] and mixing in micro channels [18].

The method of LCS studies stretching and contraction around reference trajectories. The LCS method is therefore local in nature; it provides information about invariant manifolds that determine transport in

phase space. The current method of LCS relies on computing the FTLE field using long time computations, since LCS usually can be identified only after a significant time of integration. The disadvantage of this is that, excessive stretching of line elements can introduce computational errors. Moreover specific checks on whether the stretching of line elements is within the linearized regime can be difficult to incorporate in the current algorithms on computing the FTLE. The probabilistic method on the other hand ignores the local transport structures, but using the transfer operator divides the phase space into maximally invariant sets. There have been a few attempts to explore the relationship between the geometric and probabilistic descriptions of phase space transport, such as [19] and [20]. The aim of this short paper is to present a technique of computing the FTLE using the Perron-Frobenius operator that is a step towards combining the geometric and probabilistic methods, by making the Perron-Frobenius operator the common tool to both. By utilizing the Perron-Frobenius operator to compute the FTLE, this method also strengthens the probabilistic interpretation of the FTLE, identified in [20] and [21]. This approach has the added benefits of eliminating the issue of linearization around a reference trajectory in the existing formulation of the FTLE and reduces the time to compute the FTLE field for time-dependent and periodic flows.

2 Review of FTLE and LCS

The formulation of FTLE and the Perron-Frobenius operator is reviewed in this section. This review is intended to provide an intuitive background and set the context for the computation of the FTLE using the Perron-Frobenius operator. For the rigorous definitions and details on these methods, the reader is referred to [7], [8], [4], [5], [6].

2.1 Finite Time Lyapunov exponents

Let $M \subset \mathbb{R}^n$, $\mathbf{x} \in M$ with the σ -finite σ -algebra \mathcal{B} (of Lebesgue measurable sets) and $\phi_{t_0}^t(x) : M \times \mathbb{R} \times \mathbb{R} \mapsto M$ be a flow on M . Let the associated vector field be $\dot{\mathbf{x}} = F(\mathbf{x}, t)$. Consider a reference trajectory passing through the point \mathbf{x} and a perturbed trajectory passing through the point $\mathbf{x} + \delta\mathbf{x}$ at time t_0 . The flow $\phi_{t_0}^t$ maps these points to $\phi_{t_0}^t(\mathbf{x})$ and $\phi_{t_0}^t(\mathbf{x} + \delta\mathbf{x})$ at time t and the perturbation grows to $\delta\mathbf{x}(t_0 + t)$.

Expanding $\phi_{t_0}^t(\mathbf{x} + \delta\mathbf{x})$ in a Taylor series about the point \mathbf{x} we get

$$\delta\mathbf{x}(t_0 + t) = \phi_{t_0}^t(\mathbf{x}) - \phi_{t_0}^t(\mathbf{x} + \delta\mathbf{x}) = \frac{d\phi_{t_0}^t}{d\mathbf{x}} \delta\mathbf{x}(t_0) + O(\|\delta\mathbf{x}^2(t_0)\|) \quad (1)$$

The norm or magnitude of $\delta\mathbf{x}(t_0 + t)$ can be found using the standard inner product on \mathbb{R}^n .

$$\|\delta\mathbf{x}(t)\| = \sqrt{\left\langle \frac{d\phi_{t_0}^t}{d\mathbf{x}} \delta\mathbf{x}(t_0), \frac{d\phi_{t_0}^t}{d\mathbf{x}} \delta\mathbf{x}(t_0) \right\rangle} = \sqrt{\left\langle \delta\mathbf{x}(t_0), \left(\frac{d\phi_{t_0}^t}{d\mathbf{x}} \right)^* \frac{d\phi_{t_0}^t}{d\mathbf{x}} \delta\mathbf{x}(t_0) \right\rangle} \quad (2)$$

where $*$ denotes the transpose. The maximum growth of a perturbation is therefore given by the maximum principal stretch, i.e., by the maximum eigenvalue of \mathbf{C} .

$$\max \|\delta\mathbf{x}(t)\| = \sqrt{\lambda_{\max}(\mathbf{C})} \|\delta\mathbf{x}(t_0)\| \xi_1(\mathbf{x}, t_0) \quad (3)$$

where $\mathbf{C} = \left(\frac{d\phi_{t_0}^t}{d\mathbf{x}} \right)^* \left(\frac{d\phi_{t_0}^t}{d\mathbf{x}} \right)$ is the Cauchy-Green tensor and $\xi_1(\mathbf{x}, t_0)$ is the eigenvector of \mathbf{C} associated with λ_{\max} . The growth in the perturbation depends on the initial point \mathbf{x} , initial time t_0 and the evolution or integration time $T = t - t_0$.

Definition 2.1 *The maximum FTLE is defined as, [4], [5],*

$$\sigma(\mathbf{x}, t_0, T) = \frac{1}{T} \log \left(\sqrt{\lambda_{\max}(\mathbf{C})} \right) \quad (4)$$

The leading FTLE gives the time averaged rate of stretching in a neighborhood around a reference trajectory. It is intuitively clear that regions of the phase space separated by locally high values of FTLE will stretch and separate. The sets with high FTLE act as repelling barriers in the flow. This intuitive idea of barriers is formalized by the concept of Lagrangian coherent structures (LCS), defined as ridges in scalar FTLE field, [4], [5]. Ridges can be defined precisely by appealing to differential geometric quantities as in [22], [4] and [5].

2.2 Perron-Frobenius operator

Let $B \in \mathbb{B}$ and $f \in L^1$ be a probability density function, L^1 being the space of Lebesgue measurable functions. The unique operator $P_{t_0}^t : L^1 \mapsto L^1$ defined by

$$\int_B P_{t_0}^t f d\mu = \int_{\phi^{-1}(B)} f d\mu \quad (5)$$

is called the Perron-Frobenius operator for the flow $\phi_{t_0}^t$, [23].

In practice the domain is discretized into a finite number of boxes, say $\{B_1, B_2, \dots, B_n\}$, the probability density function is approximated as a sum of simple functions on the discretized domain $f = \sum_{i=1}^N c_i \mathcal{X}_{B_i}$, where \mathcal{X}_{B_i} is the characteristic function of the set B_i , making the Perron-Frobenius operator P a linear

operator between finite dimensional vector spaces, called a stochastic transition matrix. The entries of the matrix P are determined by a Monte-Carlo simulation [7] and [8]. Each box in the domain contains a fixed number of points (initial conditions), which are integrated from a time t_0 to t . The final position of the points gives the matrix P as -

$$(P_{t_0}^t)_{ij} = \frac{\mu(B_i \cap \phi^{-1}(B_j))}{\mu(B_i)} \quad (6)$$

A time reversible operator P is required to apply the above definition for flows in forward time, [7] and [8]. This is achieved by creating a reversible Markov operator P_r given by

$$(P_{t_0}^t)_r = \frac{(P_{t_0}^t) + \overline{(P_{t_0}^t)}}{2} \quad (7)$$

where \overline{P} is the time reversed analogue of P . Its elements are given by

$$\overline{P_{t_0}^t} = \frac{u_j (P_{t_0}^t)_{ji}}{u_i} \quad (8)$$

where u_j and u_i are components of the first left eigenvector of P . For a conservative flow in which the domain is uniformly discretized, $\overline{P_{t_0}^t} = (P_{t_0}^t)^*$, the transpose of $P_{t_0}^t$. The Markov operator P has the semigroup property of $P_{t_0}^t = P_{t_0}^s + P_s^t$, where $s \in (t_0, t)$.

3 Set oriented definition of FTLE and it's computation using the Perron-Frobenius operator

The concepts of FTLE and LCS reviewed here have been used fruitfully in many areas as has been pointed out earlier. However the standard computational implementation of FTLE, using finite differences, suffers from some drawbacks, stemming from the integration time T and the linearization around reference trajectories. The method of FTLE uses the linearized flow equation (1). The evolution time $T = t - t_0$ is usually selected in a subjective fashion depending on the problem. However T has to be such that the second order terms $O(\|\delta \mathbf{x}^2(t_0)\|)$ do not grow to be too large. Usually this is accomplished by selecting a very small $\delta \mathbf{x}$ and either by keeping the time of integration T small enough or rescaling the perturbation as it grows very large. If perturbations around a specific trajectory grow too large and need to be rescaled, then additional reference points have to be introduced in that region to obtain the FTLE field at a fine enough resolution. Alternatively the computations could start with a crude mesh of initial points and refined iteratively by introducing new initial points based on the finite time stretching, requiring adaptive meshing of initial conditions, which was

explored in [15]. However the mesh refinement was not based on the size of second order terms. Moreover the stretching of line elements does not take into account folding of material lines, as shown in figure 1 which was discussed earlier in [15]. Instead of tracking only a reference trajectory and the adjacent nodes of the finite difference mesh, one tracks the movement of the whole set (shown in gray) in figure 1 and consider the distribution of points in the set, then folding and nonlinear deformation can be accounted for. A new definition of the FTLE was proposed in [20] which computed the deformation of sets instead of the stretching of line elements and partially addressed the concerns of second order terms, integration time and folding of material lines. We review the new definition here.

For illustrating the concept we assume the flow is in \mathbb{R}^2 . The method of computing FTLE using the SVD of the Cauchy-Green tensor essentially computes the stretching of a neighborhood under the action of the flow $\phi_{t_0}^t$ as shown in figure 2. The FTLE for the reference trajectory in this case is $\sigma = \frac{1}{T} \log \left(\frac{a_1}{a} \right)$ where T is the time of evolution of the trajectory.

We can treat the evolution of the set B as the evolution of two random variables X_1 and X_2 defined by a probability density function $f(x_1, x_2)$ which is initially a uniform probability density function on B given by, $f = \frac{1}{\mu(B)} \mathcal{X}_B$, where \mathcal{X}_B is characteristic function of B . The covariance matrix of f is $I_{ij} = E[(X_i - X_{im})(X_j - X_{jm})]$, with $i = 1, 2$ and $j = 1, 2$ where X_{1m} and X_{2m} are mean values of the random variables X_1 and X_2 and $E[\cdot]$ denotes the expectation $E[X_i] = \int x_i f$. Under the action of the flow $\phi_{t_0}^t$, f is mapped to Pf where P is the associated Perron-Frobenius operator.

Definition 3.1 *Let $I(f)$ be the covariance of f and $I(Pf)$ the covariance of Pf and let $\lambda_{max}(I)$ denote the maximum eigenvalue of I . Then the FTLE of B denoted by $\sigma_I(B, t_0, t)$ is defined as -*

$$\sigma_I(B, t_0, t) = \frac{1}{t - t_0} \log \left(\frac{\sqrt{\lambda_{max}(I(Pf))}}{\sqrt{\lambda_{max}(I(f))}} \right) \quad (9)$$

Since I is the covariance of f it provides a probabilistic of the FTLE. Simultaneously I can also be interpreted as the moment of inertia of the set B and provides a geometric description of the deformation or distortion of the set. In the case of linearized flow, where an initial circular blob deforms into an ellipse as shown in figure 2, the value of the covariance based FTLE is the same as that obtained from traditional FTLE calculation using line stretching.

The definition of σ_I avoids the linearization of the flow and the computation of the stretching of line elements. Further it is a set-oriented method and directly computes the deformation of a set instead of inferring it from the deformation of line elements. From computational purposes we divide the domain into boxes with a fixed number of initial points. The covariance matrix calculated for each box about its mean gives $I(f)$ and the covariance matrix calculated for Pf about its mean gives $I(Pf)$. The covariance

based method of FTLE is a bridge between the geometric approach of measuring line stretching and the probabilistic approach of almost invariant sets.

The covariance FTLE is a set oriented redefinition of the FTLE. Therefore the Perron-Frobenius operator offers a natural method to compute this FTLE, where only short time integrations are necessary. The operator $P_{t_0}^t$ can be found using a suitable set of short time intervals, $[t_0, t_1], [t_1, t_2], \dots, [t_n, t]$; $P_{t_0}^t = P_{t_0}^{t_1} P_{t_1}^{t_2} \dots P_{t_n}^t$. Let f be a uniform density function supported on a set B . Then as before $P_{t_0}^t$ maps f under the action of the flow to $P_{t_0}^t f$. For time independent flows this becomes particularly easy, with $P_{t_0}^t = (P_{t_0}^{t_0+\Delta t})^{n+1}$ where $\Delta t = t_{i+1} - t_i$ for $i = 0, 1, \dots, n$. This avoids long time integration of trajectories, which often introduces the problem of rescaling of perturbed trajectories and the growth of second order terms.

To make the discussion more concrete two dimensional flows on \mathbb{R}^2 will be considered to and P will be found by discretizing the domain into boxes, each containing a fixed number of points. The entries of the matrix $P_{t_0}^{t_0+\Delta t}$ for a suitably chosen Δt and the time reversible operator are found from equations 6, 7 and 8. To compute the FTLE over the entire domain, we take a uniform density function $u_i = [0 \ 0 \dots 1/\mu(B_i) \ 0 \ 0]$, with the i th column being equal to a constant. The vector u_i evolves to $v_i(t_0 + \Delta t)$ at $t_0 + \Delta t$, given by,

$$v_i(t_0 + \Delta t) = u_i P_{t_0}^{t_0+\Delta t} = \frac{1}{\mu(B_i)} (P_{t_0}^{t_0+\Delta t})_{ij} \quad (10)$$

Similarly the evolution of u_i at time $t = t_0 + (n + 1)\Delta t$ is given by

$$v_i(t) = u_i (P_{t_0}^{t_0+\Delta t})^{n+1} = \frac{1}{\mu(B_i)} (P_{t_0}^{t_0+\Delta t})_{ij}^{n+1} \quad (11)$$

Equation 11 gives how the set initially uniformly distributed over the box B_i is distributed at time t . Thus the covariance of this set can be found from the i th row of $(P_{t_0}^{t_0+\Delta t})^{n+1}$. Proceeding thus, the covariance FTLE for each of the boxes in the domain can be found.

It should be emphasized that the computation of the FTLE using the Perron-Frobenius operator requires a set oriented definition of the FTLE. One cannot use the operator P or its time reversible counterpart P_r to track the evolution of sets of zero measure, since the integral on the right hand side of equation 5 is zero for this case. The standard method of FTLE which requires the evolution of individual trajectories passing through the nodal points of a mesh at the initial instant of time, does not make any direct reference to sets of positive measure around these nodal points. Hence a set oriented definition of FTLE is necessary to take advantage of the Perron-Frobenius operator. In practice the computational approach for this new definition too has to make use of discrete initial conditions and trajectories, but sets of positive measure are explicitly modeled by these discrete initial conditions.

4 Examples

In this section we illustrate the computation of the FTLE using the Perron-Frobenius operator for two flows. The first is the lid-driven cavity flow studied for its mixing properties in [18] and the double gyre flow that has been a prototype flow in the LCS and almost invariant sets literature, [4, 15, 19].

4.1 Lid driven cavity flow

The problem of transport in the model of the lid driven cavity flow has been investigated in [18] and is considered here as the first example because of its simple piecewise steady velocity field. The flow is described by the stream function

$$\psi(x, y) = \sum_{n=1}^2 U_n C_n f_n(y) \sin\left(\frac{n\pi x}{a}\right) \quad (12)$$

defined on the domain $[0, a] \times [-b, b]$ for time $0 \geq t \geq \tau_f/2$. where

$$f_n = \frac{2\pi y}{a} \cosh\left(\frac{n\pi b}{a}\right) \sinh\left(\frac{n\pi y}{a}\right)$$

and

$$C_n = \frac{a^2}{2n\pi^2 b} \left[\frac{a}{2n\pi b} \sinh\left(\frac{2n\pi b}{a}\right) + 1 \right]^{-1}$$

For time $\tau_f/2 \geq t \geq \tau_f$, the sign of the velocity term U_1 is changed. This reflects the streamlines about $x = a$ after a time $\tau_f/2$.

Using symmetry arguments given in [24] and [25], a specific ratio of the magnitudes of the terms U_2/U_1 along with a fixed value of the period of the flow τ_f is found such that it generates three period-3 fixed points in the domain $[0, a] \times [-b, b]$. The specific values of the constants that we borrowed from [24] and [25] are $U_1 = -1$ and $U_2 = 0.841298$ and $\tau_f^*/2 \approx 4.740202$ for the domain $[0, a] \times [-b, b] = [0, 6] \times [-1, 1]$.

A perturbation of the time period of the flow from the critical value of $\tau_f^*/2 \approx 4.740202$ destroys the fixed points. The method of almost invariant sets was used in [26] and [18] to study mixing for different values of the perturbed time period. Since our main interest here is to illustrate the FTLE computed from the Perron-Frobenius operator, we choose a single case, a specific value of half time period $\tau_f/2 = 4.848$ for our study.

The standard FTLE computation was done for the system for different integration times that are multiples of the period τ_f , the results of which are shown in figure 3(a)-(c) by integrating points initially spaced at a distance of 0.05. The domain is then divided into 4800 boxes each box containing a 100 points and the time

reversible Perron-Frobenius matrix P_r is found by integrating a total of 480,000 initial points for a period equal to τ_f . The vector space has 120×40 dimensions which are the discretized finite approximation of the infinite dimensional space of Lebesgue integrable functions. Uniform density functions each supported on a box are the bases vectors for the finite dimensional vector space. The covariance based FTLE computation was performed using the Perron-Frobenius operator P_0^τ . Figure 3 (d) is obtained by computing the covariance of the bases functions from the rows P_0^τ , while figure 3 (e) and (f) are obtained by computing the covariance of the basis functions from the rows of $P_0^{2\tau} = (P_0^\tau)^2$ and $P_0^{3\tau} = (P_0^\tau)^3$ respectively.

It is evident from the figure 3 that the FTLE field has the same ridge structure when computed by the line stretching approach or the covariance approach using the Perron-Frobenius operator. Computing the covariance based FTLE field directly by integrating all the initial conditions to 3τ , while more accurate is computationally more intensive. In fact the time taken for this method increases almost linearly with the integration time. The FTLE field computed from the Perron-Frobenius operator has the same features as the covariance FTLE field by integrating the points in each of the boxes for 3τ and computing the covariance of the bases functions which is shown in figure 4.

While the FTLE field computed directly by integration and that computed by the Perron-Frobenius operator have the same ridge features, they differ in the magnitude of the FTLE field. This discrepancy in the magnitude is due to the approximation of the Perron-Frobenius operator by a matrix. This approximation introduces errors in the computation of the covariance matrix. As shown in figure a uniform density function, f , with a measure m is mapped to Pf whose support lies on four boxes B_1, B_2, B_3 and B_4 . This is approximated by four uniform density functions supported on the four boxes respectively whose measures are $m_i = m(\text{supp}(Pf) \cap B_i)/m$, where $\text{supp}(Pf)$ is the support of the function Pf and $i = 1, \dots, 4$. The mean and the covariance due to the four uniform density functions is only an approximation of the mean and the covariance of the function Pf . The approximation of the Perron-Frobenius operator by its finite dimensional counterpart thus leads to errors in the covariance of the function Pf about its mean. As the box size in the computation is reduced and the matrix size increased, it is natural to expect that the matrix approximation of P and the covariance computation become more accurate, though no rigorous proof is offered here.

4.2 Double gyre flow

The double gyre flow which is time dependent but periodic, has been one of the prototype flows in the LCS literature, [4], [19]. The double gyre flow is defined by the stream function $\psi(x, y, t) = A \sin(\pi f(x, t)) \sin(\pi y)$, with the parameters $A = 0.1$, $\omega = 0.2\pi$ and $\epsilon = 0.25$. The time period of the flow is $\tau = 1$. The domain is discretized into 50000 square boxes of size 0.005 each containing 625 points. The FTLE field computed

using the stretching of line elements and the FTLE field computed from the Perron-Frobenius operator is shown in figure 6.

As observed in the discussion on the lid driven cavity flow, the FTLE field has the same ridge features, when the covariance of the sets Pf are computed directly by integrating all the points in each box to $T = 10$, as shown in figure 7 and when computed using the Perron-Frobenius operator. Moreover because of the more accurate approximation of the domain by a higher number of boxes, the covariance FTLE field computed by a direct integration and that computed by the Perron-Frobenius operator are closer to each other in magnitude.

5 Conclusion and Discussion

A method to compute the FTLE field using the Perron Frobenius method has been introduced in this paper. To do this a modified definition of the FTLE was used which identifies deformation of sets of positive measure instead of the stretching of line elements. This methodology is general enough to be used in time-dependent flows and is particularly useful in the case of time-independent and periodic flows, where it offers a significant computational advantage by eliminating long time integrations. The standard approach of computing the FTLE field has some shortcomings because of the tangent linearization. The covariance based method of computing the FTLE does not use the linearized equations of a flow making it more general in scope of application. The method of computing the covariance FTLE was illustrated by two examples; the lid driven cavity flow and the double gyre flow. In both cases it was shown that the FTLE field computed by the new method has the same topological features as the FTLE field computed using the standard approach of line stretching. Moreover the covariance FTLE gives the deformation of sets a probabilistic interpretation. The new method of computing the covariance FTLE introduced in this paper is based on the Perron-Frobenius operator; a common tool in probabilistic methods of phase space transport. This puts the Perron-Frobenius operator at the center of study of phase space transport. This is perhaps intuitively obvious since the Perron-Frobenius operator contains all the information of global transport of sets. The method of computing the covariance FTLE using the Perron-Frobenius operator is a significant step in combining the probabilistic and geometric methods of phase space transport, into a common unified framework.

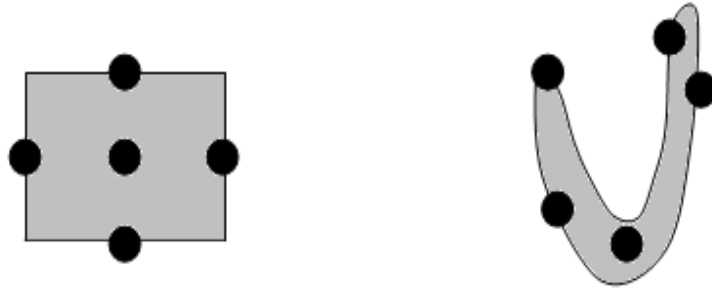


Figure 1: Folding of material elements.

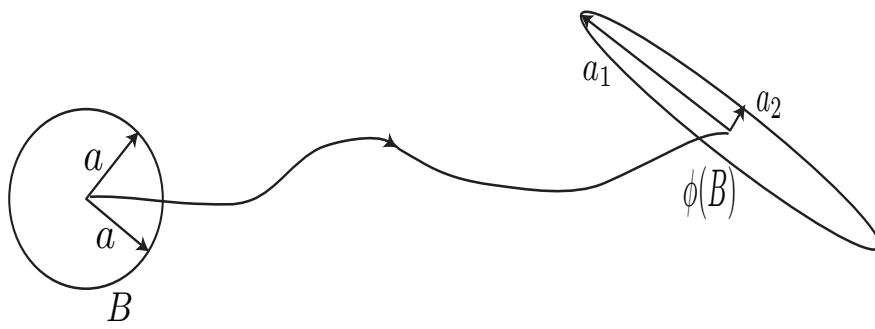


Figure 2: Deformation of a blob under the flow

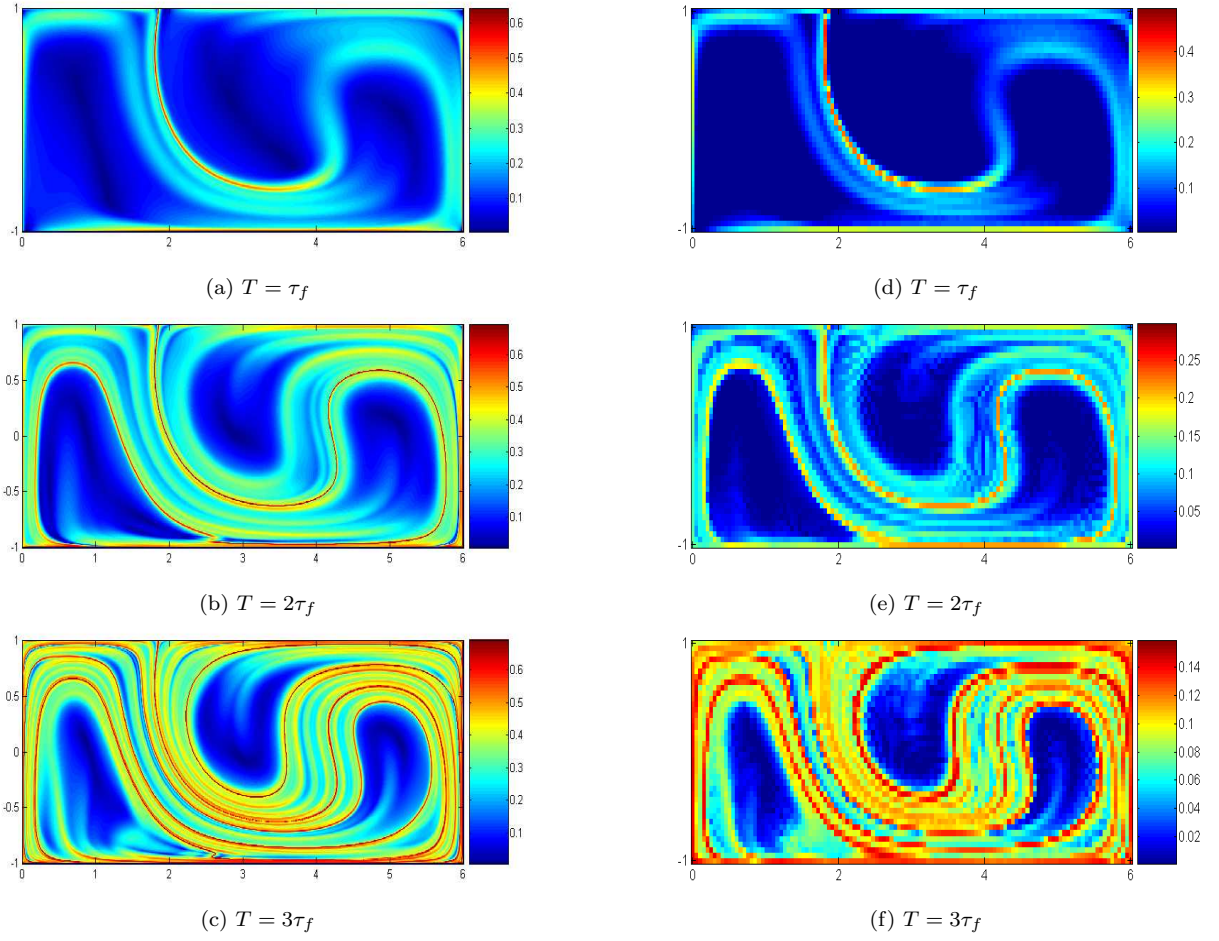


Figure 3: FTLE for integration time T for the lid driven cavity flow.

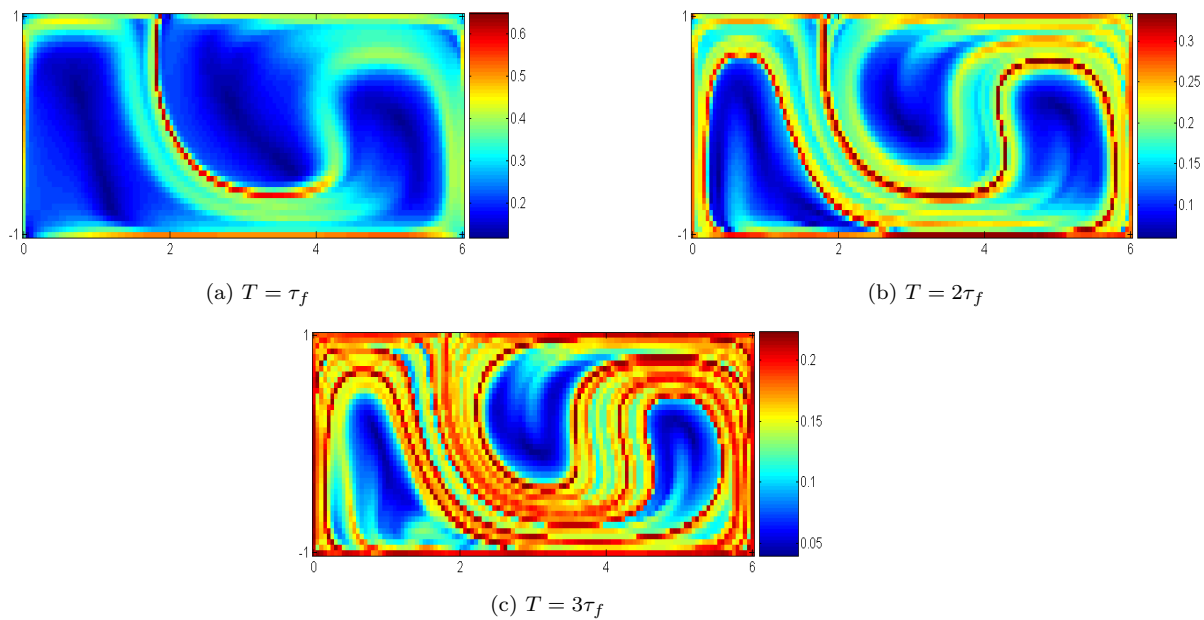


Figure 4: Covariance FTLE for lid driven cavity flow computed by direct integration of initial conditions for various integration times.

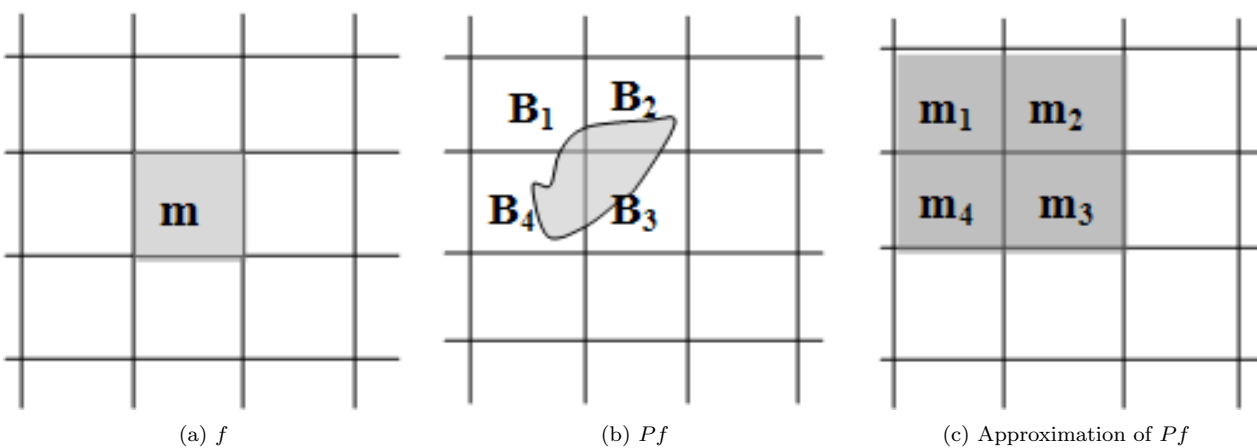


Figure 5: Error in the computation of covariance introduced by the approximation of the Perron-Frobenius operator.

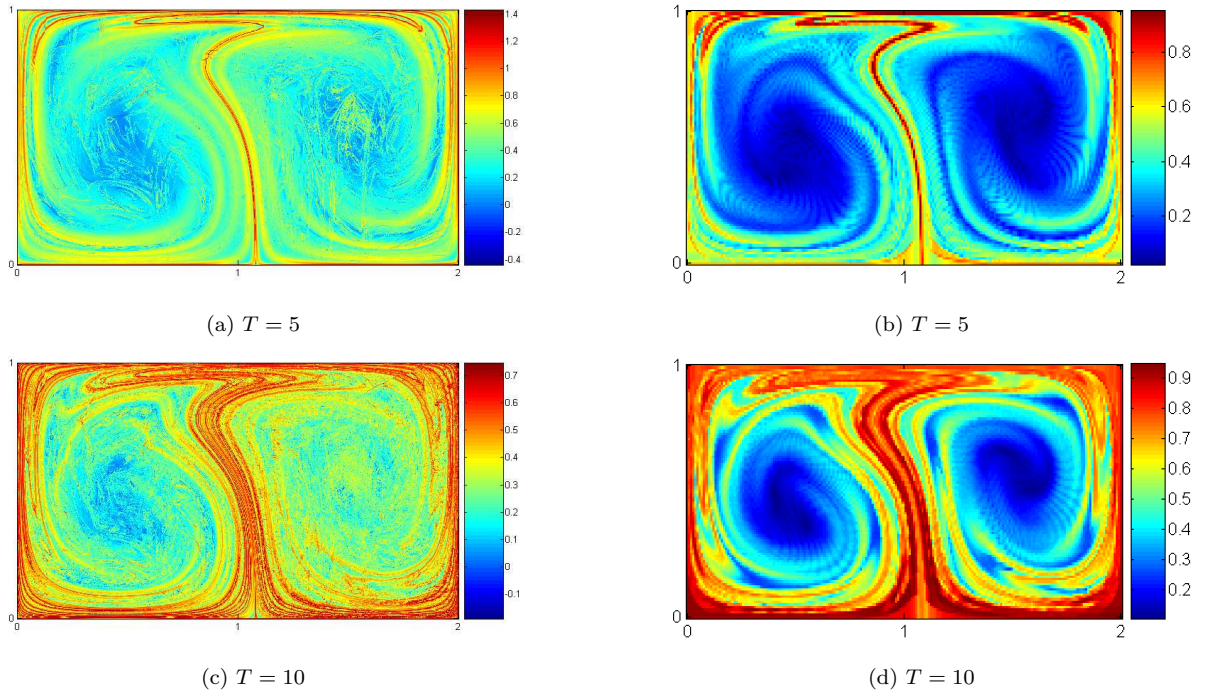


Figure 6: FTLE for integration time T for the double gyre flow.

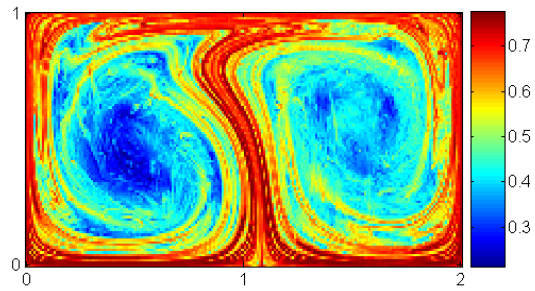


Figure 7: Covariance FTLE obtained by direct integration for an integration time $T = 10$ for the double gyre flow.

References

- [1] S. Wiggins, Chaotic transport in dynamical systems, IAM, Springer, first edition edition (1993).
- [2] K. Ide, D. Small and S. Wiggins, Nonlinear Processes in Geophysics, (**9**), 237 (2002).
- [3] S. Wiggins, Annual Review of Fluid Mechanics, (**37**), 295 (2005).
- [4] S. C. Shadden, F. Lekien and J. Marsden, Physica D, (**212**), 271 (2005).
- [5] F. Lekien, S. C. Shadden and J. Marsden, Journal of Mathematical Physics, (**48**), 065404 (2007).
- [6] G. Haller, Physics of Fluids A, (**13**), 3368 (2001).
- [7] M. Dellnitz and O. Junge, SIAM Journal on Numerical Analysis, (**36**), 491 (1998).
- [8] G. Froyland and M. Dellnitz, SIAM Journal on Scientific Computing, (**24**), 1507 (2009).
- [9] G. Froyland, S. Lloyd and N. Santitissadeekorn, Physica D, (**239**), 1527 (2010).
- [10] G. Froyland, N. Santitissadeekorn and A. Monahan, Chaos, (**20**), 043116 (2010).
- [11] P. C. Du Toit, PhD thesis, California Institute of Technology (2010).
- [12] C. Coulliette, F. Lekien, J. D. Paduan, G. Haller and J. Marsden, Environmental Science and Technology, (**41**), 6562 (2007).
- [13] P. Tallapragada and S. D. Ross, Physical Review E, (**78**), 036308 (2008).
- [14] G. Haller and T. Sapsis, Physics of fluids, (**20**), 017102 (2008).
- [15] F. Lekien and S. D. Ross, Chaos, (**20**), 017505 (2010).
- [16] W. Tang, M. Mathur, G. Haller, D. C. Hahn and F. H. Ruggiero, Journal Atmospheric Science, (**67**), 2307 (2010).
- [17] M. Wilson, J. Peng, J. O. Dabiri and J. D. Eldredge, Journal of Physics: Condensed Matter, (**21**), 204105 (2009).
- [18] M. Stremmer, S. Ross, P. Grover and P. Kumar, Preprint PRL (2010).
- [19] G. Froyland and K. Padberg, Physica D, (**236**), 1839 (2003).
- [20] P. Tallapragada and S. D. Ross, Preprint (2010).
- [21] P. Tallapragada, PhD thesis, Virginia Polytechnic Institute and State University (2010).

- [22] D. Eeberly, *Ridges in Image and Data Analysis*, Kluwer Academic Publishers, second edition (1996).
- [23] *Chaos, Fractals and Noise : Stochastic Aspects of Dynamics*, Springer-Verlag, second edition (1994).
- [24] J. Chen and M. A. Stremler, *Phys. Fluids* (**21**), 021701 (2009).
- [25] M. A. Stremler and J. Chen, *Phys. Fluids* (**19**), 103602 (2007).
- [26] P. Grover, PhD thesis, Virginia Polytechnic Institute and State University (2010).